

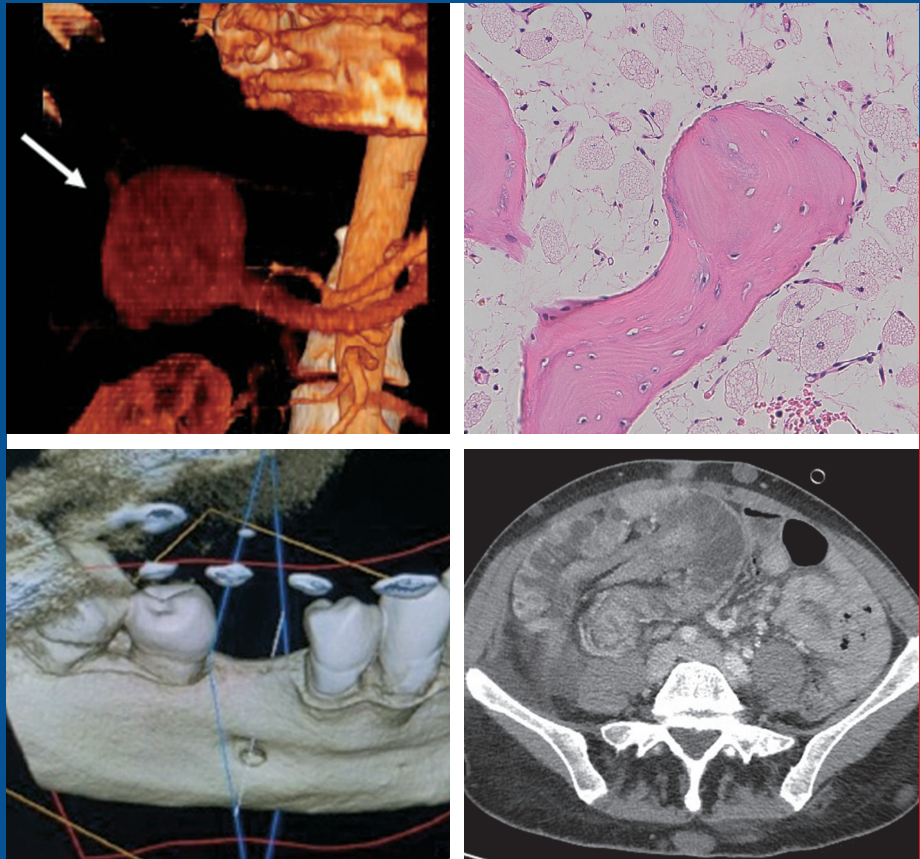


Società Italiana  
di Radiologia Medica  
e Interventistica

# Journal of **RADIOLOGICAL REVIEW**

**Editor in Chief**  
**ANTONIO PINTO**  
*Napoli, Italy*

Spedizione - Poste Italiane S.p.A.



VOLUME 9 • NUMBER 3  
SEPTEMBER 2022

EDIZIONI MINERVA MEDICA

# Cone beam computed tomography-controlled osteotomy: safety in implantology

Vittorio GILMOZZI <sup>1</sup>, Simona CESARI <sup>1</sup>, Francesco TUCCI <sup>2</sup> \*, Francesco MONTEDURO <sup>2</sup>

<sup>1</sup>Private practitioner, Bologna, Italy

<sup>2</sup>Department of Radiology, IRCCS Sant'Orsola Hospital, Bologna, Italy

\*Corresponding author: Francesco Tucci, Department of Radiology, IRCCS Sant'Orsola Hospital, Via Giuseppe Massarenti, 9, 40138 Bologna, Italy.  
E-mail: francesco.tucci5@studio.unibo.it

DOI: 10.23736/S2723-9284.22.00200-X

## ABSTRACT

**BACKGROUND:** Difficult osteotomy is one of the most frequent issues in implantar surgery, that arises even for the most experienced implantologists. Other imaging techniques such as endoral XR, videoradiography and panoramic tomography help to control the implant's orientation after surgery but are not sufficient in evaluating all the sinuses and recesses in the oral cavity.

**METHODS:** The authors analyzed 205 implantations that were carried out over three years. One of the most frequent problems related to Cone Beam CT is represented by the scattering effect, and this was overcome designing stainless radiopaque references, whose diameter is set on the dimensions of the milling cutter used. Moreover the CBCT were performed in lowdose mode, according to the radiological exposure guidelines.

**RESULTS:** Compared to other radiological techniques, the CBCT control provides the surgeon with a tridimensional reconstruction that helps to preserve the integrity of fragile anatomical structures such as the inferior alveolar nerve and to perform osteotomy in areas that are difficult to approach. The images obtained thanks to this protocol are pivotal both to program the implantar surgery and to carry out intraoperative controls.

**CONCLUSIONS:** The technique shown in this article makes the osteotomy outcome totally predictable and helps the surgeon to correct the inclination of the axis whether necessary.

(Cite this article as: Gilmozzi V, Cesari S, Tucci F, Monteduro F. Cone beam computed tomography-controlled osteotomy: safety in implantology. J Radiol Rev 2022;9:122-32. DOI: 10.23736/S2723-9284.22.00200-X)

**KEY WORDS:** Osteotomy; Cone-beam computed tomography; Safety.

This article is about a new operatory flow chart, that the authors called cone beam computed tomography (CBCT) controlled osteotomy. CBCT controlled osteotomy is intended to make implant's outcome totally predictable, even in the areas that are very difficult to approach from an anatomical point of view (Figure 1).<sup>1</sup>

Performing an intraoperative CBCT control enables the sur-

geon to carry out implantar surgery both with a bone flap and with the flapless technique, even in areas whose anatomical features may cause an unsuccessful osteotomy (Figure 2).<sup>2</sup> During the operatory phases, it is possible to use directional steel pins, that are frequently available in the common surgical kits. The pins help to control which the implantar preparation's orientation is, thanks to analogical or digital radio-

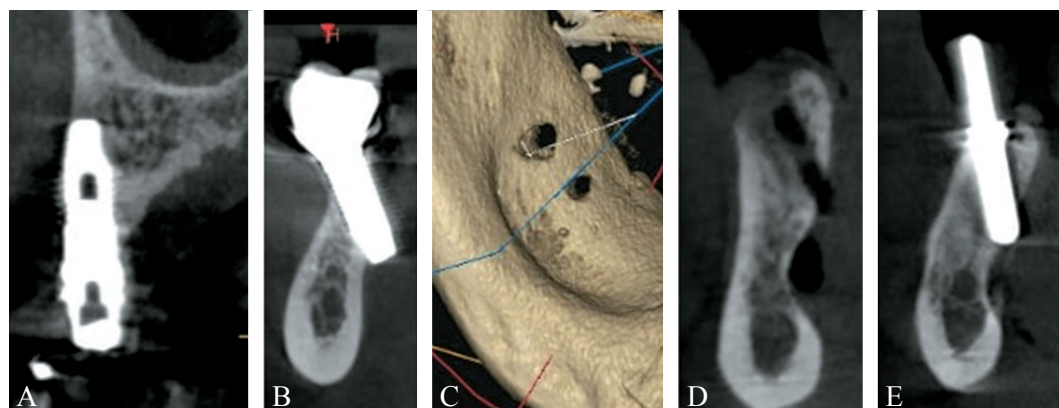


**Figure 1.**—Some examples of perfectly carried out osteotomies, in axis with the natural corono-radicular course of adjacent teeth, that does not reach the cortical bone.



**Figure 2.**—Steel pin safely placed in the osteotomy.



**Figure 3.**—Steel pin safely placed in the osteotomy, apparently in line with the occlusal plane.

logical techniques (endoral XR, videoradiography, phosphate film and panoramic tomography). On the other hand it is not possible to guarantee safety in vestibular-lingual or palatine direction (Figure 2, 3).

This study is intended to describe a new surgical technique that introduces the CBCT within the surgical phases, in order to optimize the osteotomy inclination and to respect the maxillary bone's anatomy as much as possible.

The authors demonstrate that this technique enhances the success predictability<sup>3</sup> and ensures a better surgical safety both to the neophyte surgeon and to the most experienced implantologist (Figure 4).

Using CBCT during surgery enables the implantologist to correct the osteotomy inclination, granting a predictable implant-prosthetic rehabilitation. This achievement is especially useful

in cases that result very complex from an anatomical point of view, but can ensure a better result even in simpler cases.

The CBCT controlled osteotomy technique is pivotal in cases where it is mandatory to study the amount of available bone in the three plane of space in order to insert the implant as safely as possible.<sup>4</sup>

In order to describe the evolution of the technique presented in this article, we plan to insert an implant in position 45. It can be seen that it is not possible to evaluate the inferior alveolar nerve course if we use a VRG or a preoperative panoramic tomography (Figure 5A, B).

Thanks to several CBCTs the implant placement can be planned (Figure 6A, B) behind the nerve's pathway and its emergence, that is located in a vestibular position and appears to be quite thick (Figure 7A, B).

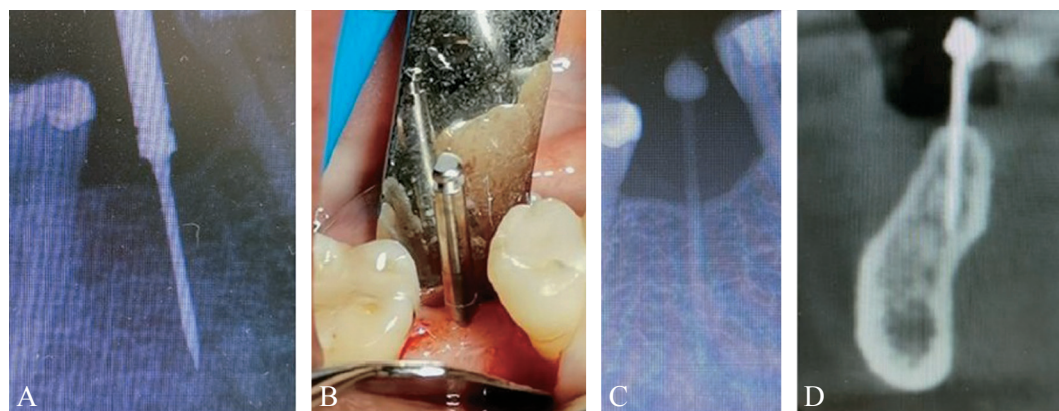


**Figure 4.**—A) VRG showing the position of an osteotomy carried out with a lanceolate milling cutter (1.1 mm); B) surgical field with lanceolate milling cutter in the vestibular area; C) VRG control carried out with radiopaque reference (0.1 mm); D) the lowdose CBCT control, carried out with the same radiological reference, shows that it is necessary to correct the inclination axis of the osteotomy.



**Figure 5.**—Both the OPT (A) and the VRG (B) do not show the IAN pathway and emergence.

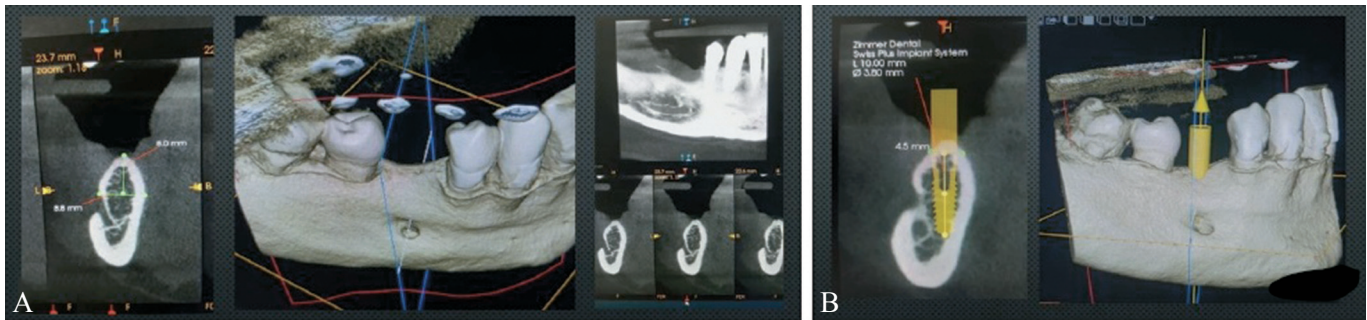


**Figure 6.**—A) Preoperative CBCT; B) implant planning with the aid of a CBCT.



**Figure 7.**—A) CBCT control (scattering occurs with the Zimmer Biomet TMM4B11 Trabecular implant); B) VRG control (no scattering occurs).

At the beginning the authors used steel pins inserted in the osteotomy, then they verified the inclination of the preparation using an intra operative CBCT (Figure 8).

Steel pins resulted inappropriate because they helped to identify the directional axis of the preparation itself, but were not useful in taking measurements of the osteotomy and its distance from the anatomical references with millimetrical precision: in fact the radiological imaging appeared to be inaccurate because of the scattering artifact caused by the metallic material.<sup>5</sup>

In order to remove this kind of artifact the authors designed some radiopaque references that can faithfully reproduce the dimensions and the shape of the milling cutter used during the osteotomy (Figure 9).

### Materials and methods

The authors designed radiopaque pins to be inserted in the osteotomy in order to prevent the scattering artifact while the intraoperative CBCT is carried out, in order to obtain a precise volume measurement of the just performed osteotomy. These pins are made of a self-photo polymerized resin and a fiberglass core and can be autoclaved at 121 °C repeatedly. The pins underwent a further thermo-polymerization in order to ensure the resin stability.



**Figure 9.**—At the beginning of this research the authors reproduced the steel pins produced by Zimmer Biomet using a fiberglass and composite resin material. This pin had a double diameter of 2.3 and 2.8 mm, as the original one.

**Figure 8.**—CBCT with sectorial FOV performed after the insertion of a 2.8-mm steel pin in the osteotomy. It is easy to notice the scattering occurrence.





**Figure 10.**—The authors realized these radiopaque pins increasing diameter (1.0 mm; 1.8 mm; 2.2 mm; 2.7 mm), that were provided with a safety hole .



**Figure 11.**—The different milling cutters used throughout the study and their increasing diameter (1.1 mm; 1.9 mm; 2.3 mm; 2.8 mm).

The glassfiber core is intended to reinforce the pins to prevent them from twisting during the sterilization cycle and their rupture during the surgical phases.<sup>6</sup> The pins have a tolerance range of their diameter of 0.1 mm in relation to the diameter of the milling cutter used.

In order to standardize the process the authors designed four different pins with increasing diameter: 1.0 mm; 1.8 mm; 2.2 mm; 2.7 mm (Figure 10).

The milling cutter diameter used during the osteotomy equals the pin's diameter, with a 0.1 mm tolerance range to allow their passive placement in the osteotomy (Figure 11).

If necessary, we can correct the osteotomy with a larger milling cutter (1.9 mm), that is followed by a new CBCT control with the 1.8 mm pin inserted into the osteotomy.

It is important to remarke that the pins are firmly tied in order to prevent the patient from swallowing them accidentally while the CBCT is carried out<sup>7</sup> (Figure 12).

Then, if the inclination needs correction, it is possible to perform a further adjustment of the osteotomy with 2.3 mm and 2.8 milling cutters, followed by CBCT controls carried out respectively with 2.2 mm and 2.7 mm radiopaque references. The authors use two lanceolate milling cutters of different lengths, whose working part is respectively 12 mm and 17 mm long.

Whether the surgeon is confident about the osteotomy inclination, he can decide to use a limited number of milling cutters, lowering, therefore, the patient radiological exposure.

This study involves parasagittal plates only, that appear in 5 different 1 mm sections: these images are produced thanks to the Dicom<sup>®</sup> feature "split sight." This working method helps to plan the surgery and to carry out controls during the surgery, using the sagittal cutting feature. This approach is portrayed in the following figures (Figure 13-16).

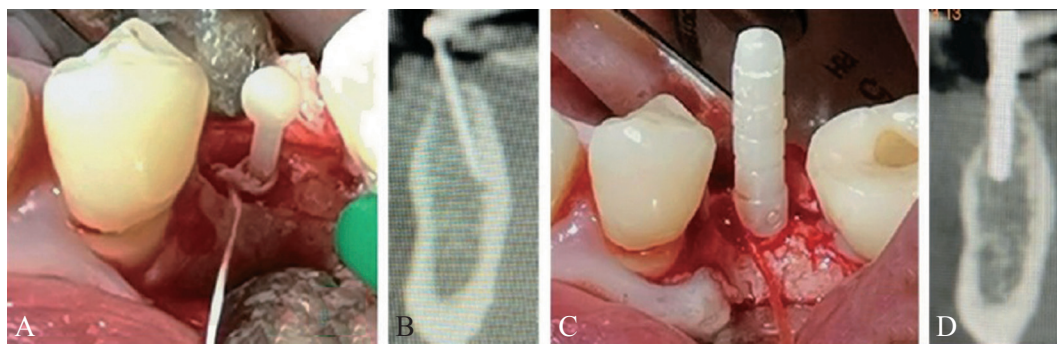


**Figure 12.**—A) 1.0 mm diameter pin safely placed; B) CBCT control; C) 2.3 mm diameter pin safely placed; D) the CBCT control shows the osteotomy axis after the surgical correction.

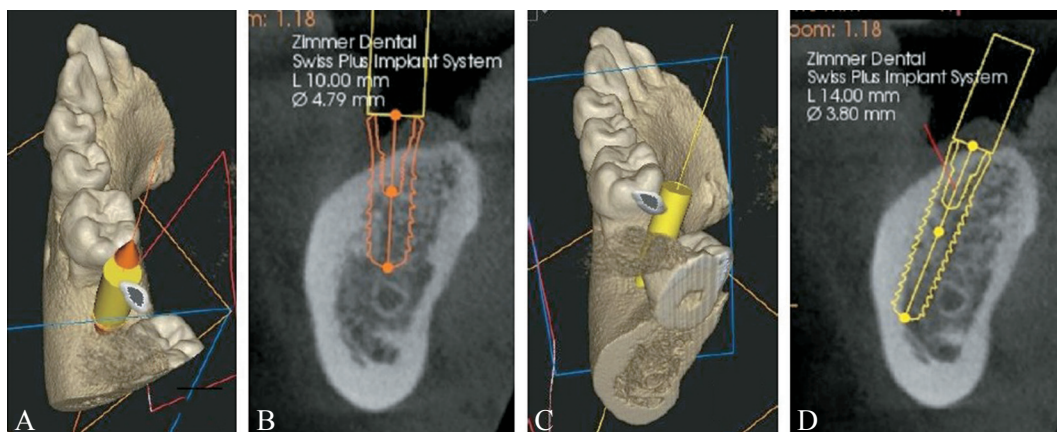


**Figure 13.**—A) Panoramic 3D reconstruction showing the nerve section emergence planned in 37, in axis with adjacent teeth; B) parasagittal plane and implant planning in 37 with Zimmer Biomet SPMB10; C) 3D panoramic with the nerve emergence that was planned in 37 in a more lingual position compared to adjacent teeth; D) parasagittal plane showing a Zimmer Biomet SPMB14 implant to be performed with a CBCT control.

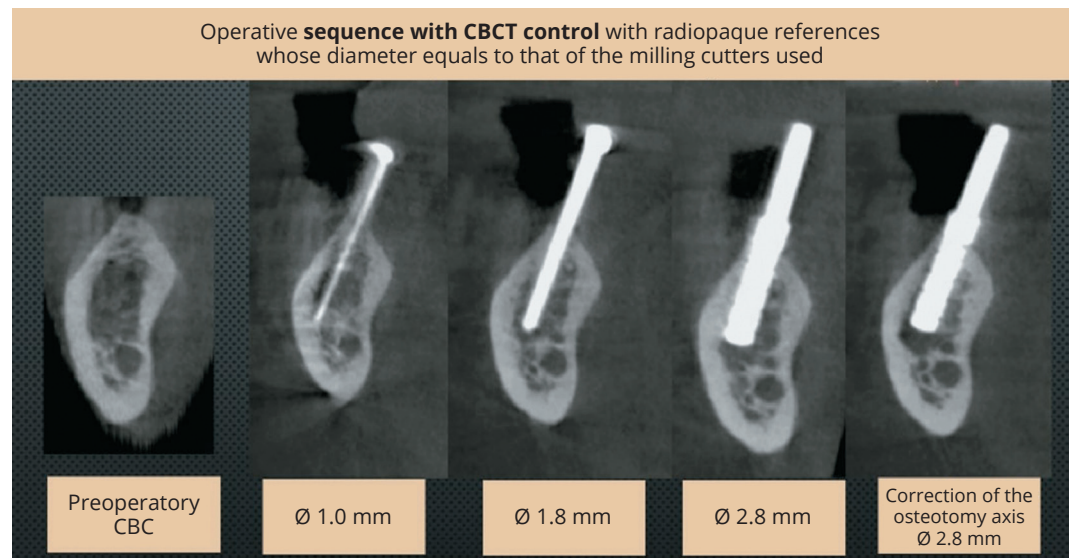


**Figure 14.**—A sequence of sectorial intraoperative CBCTs with pins with increasing diameter.

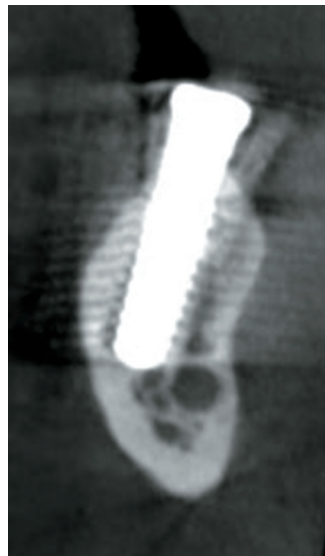


**Figure 15.**—Zimmer Biomet SPMB12 placed before the IAN pathway thanks to CBCT control.

**Results**

All patients enrolled into this study were informed about its goal and signed a specific consent form for the intraoperative CBCT.

The CBCT controlled implantations were performed within three years (Table I); 205 implants were placed and 113 of

**Table I.**—Pool of patients treated with CBCT controlled osteotomy in 2019, 2020 and 2021.

CBCT controlled osteotomy	Superior arch	Lower arch
Male	48	45
Female	65	47
Metallic pins	50	62
Radiopaque pins	42	51
Flapless	43	19
Flap	70	73

them at the superior maxillary bone (65 in female patients and 48 in male patients) and 92 at the mandibular bone (47 in female patients and 45 in male patients). All patients ranged from 27 to 85 years; 93 implantations were performed with steel pins and 112 implantations were performed with radiopaque resin pins. Sixty-two cases were carried out with the flapless technique (43 at the maxilla, 19 at the mandible); 143 cases were performed using a bony flap (70 at the maxilla and 73 at the mandible).

Using steeless pins makes it possible to perform radiological controls, setting the CBCT in sectorial lowdose mode with a

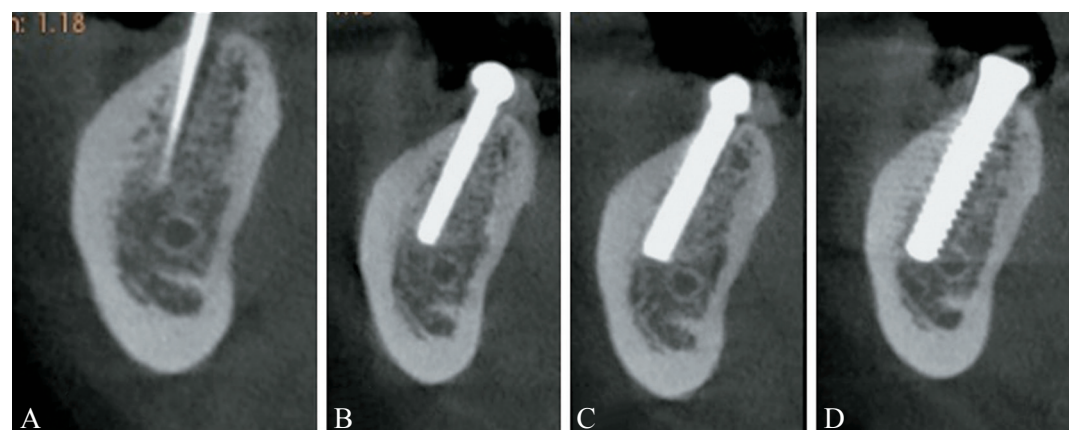


**Figure 16.**—Complete sequence of intraoperative CBCTs carried out in sectorial mode with a reduced FOV. A) Radiopaque Ø 1.0 mm reference; B) radiopaque Ø 2.2 mm reference; C) radiopaque Ø 2.7 mm reference; D) post-operative CBCT control.

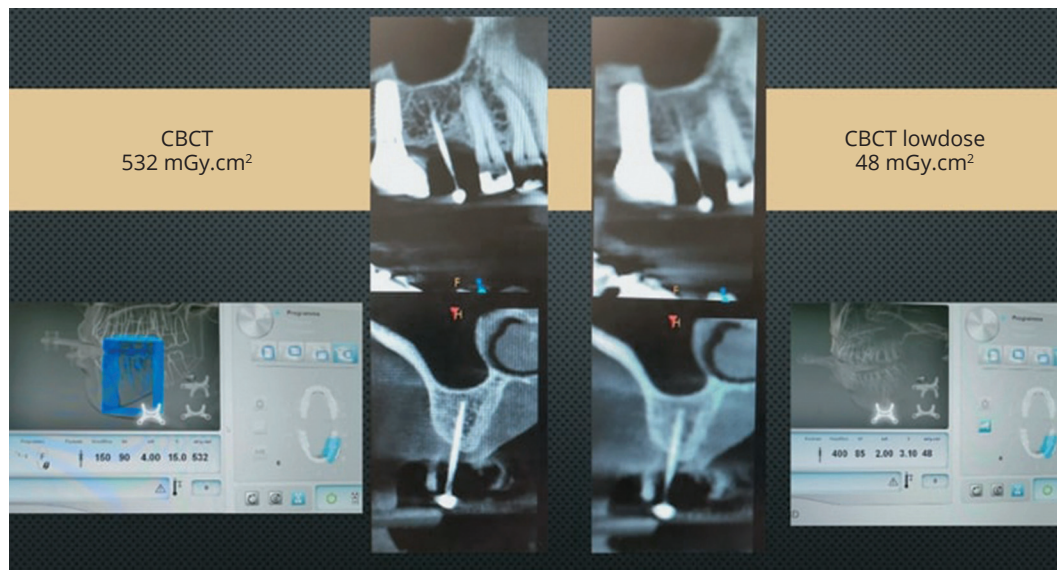


**Figure 17.**—Intraoperative sectorial CBCTs compared: standard mode vs. lowdose mode.

reduced FOV (field of view), this precaution reduces the patient exposure from 532 mGy/cm<sup>2</sup> to 48 mGy/cm<sup>2</sup> (Figure 17). Thanks to the radiopaque nonmetallic pins it is possible to prevent scattering artifacts, thus the CBCT controls were carried out with a lowdose in order to expose the patient to a dose of only 48 mGy/cm<sup>2</sup>.

As shown in the pictures, the target area appears clear even if we exposed the patient to a very small amount of radiation if compared to a normal CBCT. Scattering occurs even in CBCT controls carried out after surgery and provides the implantologist with a clear and precise image of the implant borders and from, that helps to measure the distance between the implant itself and the cortical bones or the nerve's pathway. In fact, scattering always makes the implant's length and diameter look oversized.

Once the first osteotomy is performed with a lanceolate milling cutter, a radiopaque 1.0 mm pin is inserted into the osteotomy itself and the first intraoperative CBCT is carried out. Then, if the inclination needs correction, it is possible to perform a further adjustment of the osteotomy with 2.3 mm and 2.8 mm milling cutters, followed by CBCT controls carried out respectively with 2.2 mm and 2.7 mm radiopaque references. The authors use two lanceolate milling cutters of different

lengths, whose working part is respectively 12 mm and 17 mm long.

Whether the surgeon is confident about the osteotomy inclination, he can decide to use a limited number of milling cutters, lowering, therefore, the patient radiological exposure.

## Discussion

Thanks to the intraoperative CBCT controls it is possible to insert an implant even in areas surgically difficult to approach, *e.g.*, the tuber maxillae and the sinu-maxillary recess, that is found in most of the patients in the posterior area and can be more or less pronounced due to the individual anatomical variability (Figure 18).

The authors analyzed more than 200 parasagittal CBCT of the maxilla in its posterior area, finding out that this recess can be defined by the cortical of the maxilla and the cortical of the pavement of the sinus; in other cases, we can find out a tri-cortical configuration, that involves the cortical of the pavement of the nasal bone too (Figure 18B).

This recess can be used whether the surgeon wants to insert an implant in a bone with an hypertrophic Schneider's membrane or

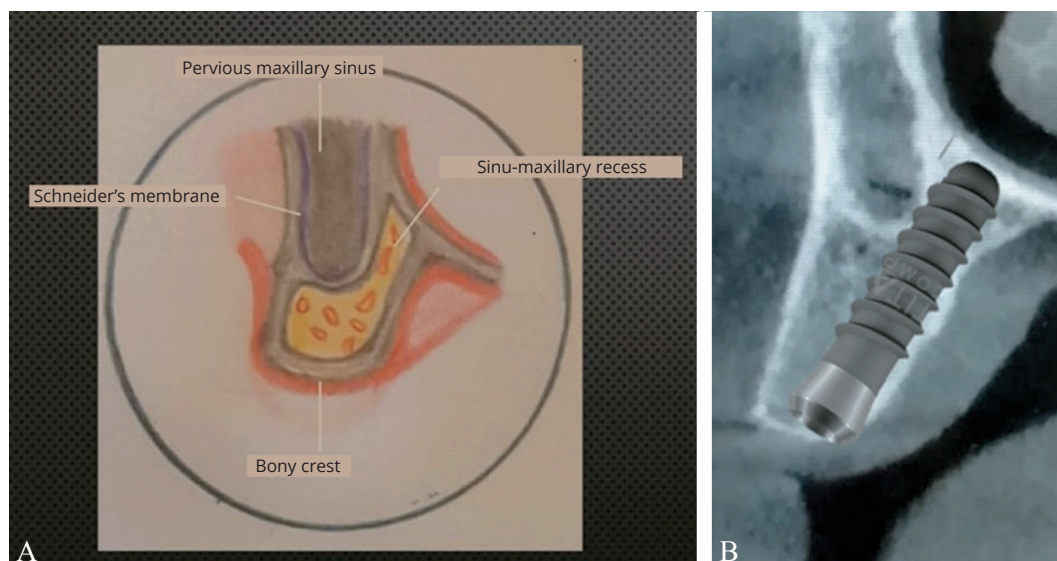


**Figure 18.**—A) Anatomical illustration by the authors - parasagittal projection that highlights the sinu-maxillary recess; B) preoperative planning that takes advantage of the tri-cortical structure in the sinu-maxillary-nasal area.

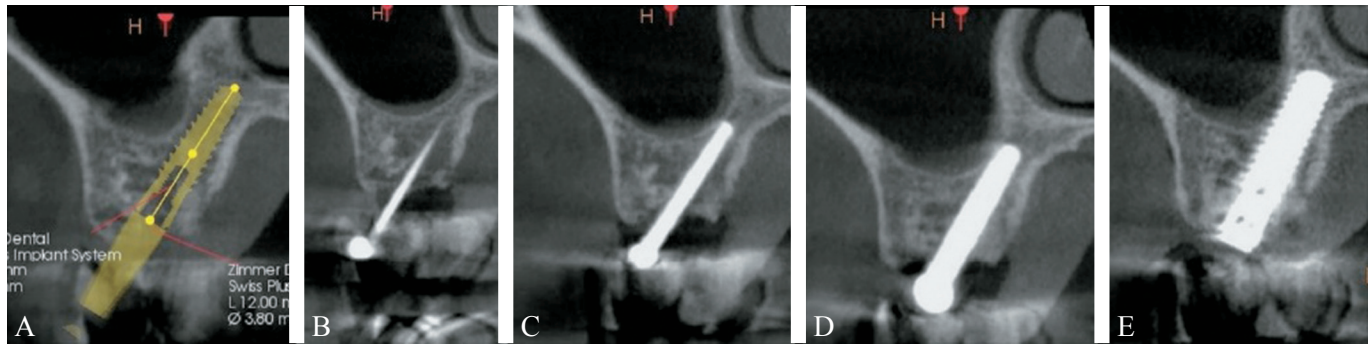


**Figure 19.**—A sequence of intraoperative CBCTs used to approach areas that can not be reached with the standard techniques. A) Preoperative CBCT used to plan the surgery; B) radiopaque Ø 1.0 mm reference *in situ*; C) radiopaque Ø 2.2 mm reference *in situ*; D) radiopaque Ø 2.7 mm reference *in situ*; E) postoperative CBCT (Zimmer Biomet SPMB12).

lacking patency of the ostium, that would contraindicate the use of particulate filler.<sup>8,9</sup>

In the following case it is shown how the intraoperative CBCT highlighted the necessity to correct the osteotomy axis in order to insert an implant in the area n.16 in the sinu-maxillary recess (Figure 19).

The next case is about a patient that went through her first visit with the implant edge having a fracture in position 15. The intraoperative CBCT allowed both the fragment removal and the insertion of the implant during the same operation (Figure 20, 21).

To this purpose osteotomy was carried out tilting the insertion axis in order to re-create the bicortical sinu-maxillary surface. The tuber maxillae is another part quite difficult to approach during surgery. The authors show that it is possible to make a better osteotomy of the tuber thanks to this technique, that helps not to damage the cortical part of the bones (Figure 22).

It can be seen that only one lanceolate 1.1 mm milling cutter was sufficient to check the osteotomy inclination. Whether the surgeon is sure about the osteotomy axis and this is confirmed by a CBCT, it is possible to reduce the number of milling cutters to use.

Due to the radiation exposure principle (59/2013/EURATOM, art. 6, par. 1,2, art. 19, par. 4, 55; DL. 26/05/2000, n. 187, art. 3) all the individual exposures need prior consent, taking into account the goals of the exposure and the individual characteristics of the person involved.<sup>10</sup> The radiological exposure during a sectorial intraoperative CBCT in lowdose mode equals to 48 mGy/cm<sup>2</sup>, thus a patient that undergoes osteotomy is exposed up to 6 CBCT, including both the preoperative and the postoperative ones, if this protocol is applied.<sup>11</sup>

According to the DL. del 31/07/2020, the limit for effective dose shall be 1 mSv in a year,<sup>10</sup> provided that the effective dose is quantified in Sievert (Sv) and each Sv equals to one Gray (Gy).<sup>12</sup>

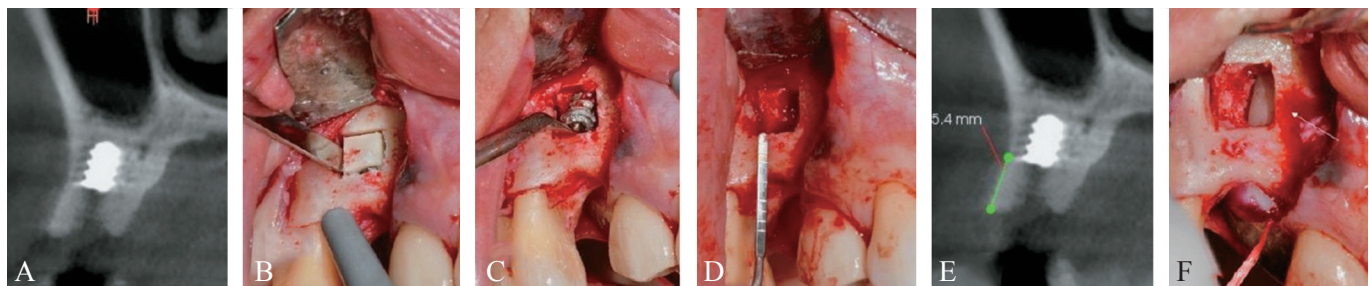


**Figure 20.**—A) preoperative CBCT; B) preparation of the vestibular bone window with piezo-surgery and removal of the cortical bone; C) removal of the fractured edge of the implant; D) the periodontal probe shows the congruence of the clinical features and the radiological images; E) preoperative CBCT that shows the correct distance between the bony ridge and the base of the vestibular window that will be performed; F) osteotomy with a 2.8 mm milling cutter and CBCT control with 2.7 mm radiopaque reference that can be seen from the bony vestibular window.

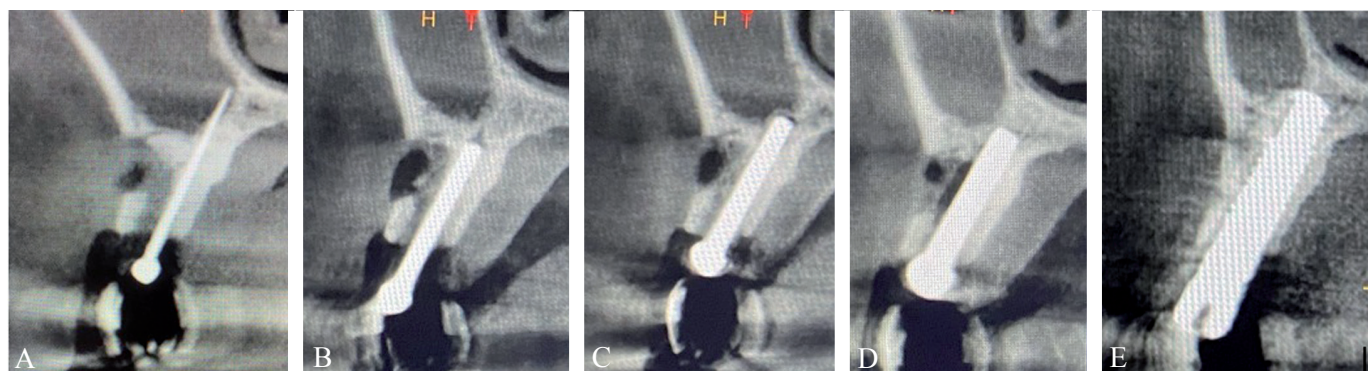


**Figure 21.**—Sequential sectorial intraoperative lowdose CBCTs, with references with increasing diameters (1.0 mm; 1.8 mm; 2.2 mm; 2.7 mm); postoperative CBCT control (Zimmer Biomet SPMB14).

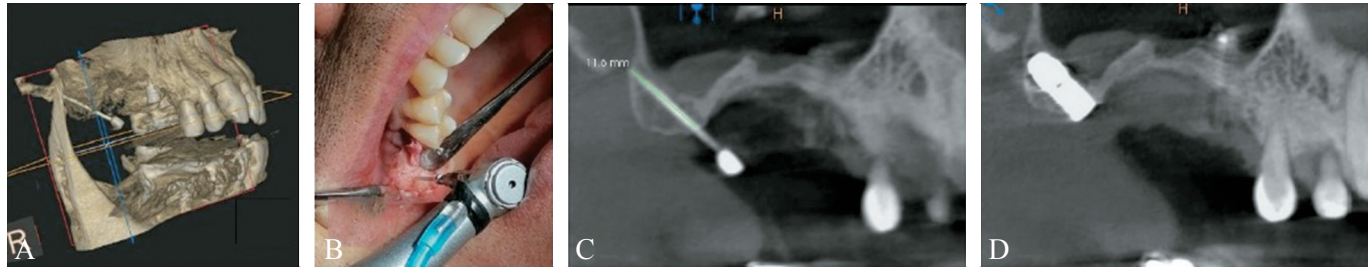


**Figure 22.**—A) Intraoperative 3D panoramic with radiopaque 1.0 mm reference; B) osteotomy inclination with a lanceolate 1.1 mm milling cutter; C) sectorial intraoperative lowdose CBCT with a 1.0 mm radiopaque reference; D) postoperative CBCT control with Zimmer Biomet TMM4B11 Trabecular.

The authors show that this protocol exposes patients to a radiation dose lower than 0.002 mSv, according to the radioprotection article published in Gazzetta Ufficiale della Repubblica Italiana (12/08/2020).<sup>13</sup>

Furthermore the authors demonstrate that the radiation exposure principle is respected in this protocol thanks to nonmetallic pins (59/2013/EURATOM, art. 22, point c, and art. 56; 26/05/2000, n. 187, art. 4) and it involves the exam quality control and the patient exposure evaluation.<sup>14</sup> These pins, in fact, prevent the scattering and the authors could perform clear and precise CBCTs even in lowdose mode. Given this, it is possible to claim that a CBCT controlled osteotomy implies the patient exposure to a dose that is lower than the one involved in a CBCT performed over the whole dental arch and with the full dose.<sup>13</sup>

In the end, the authors prove that the CBCT osteotomy is optimal even in the most complex cases. The following case

report is intended to show how this approach allows to insert eight implants into an edentulous maxillary bone of a 79 years old female patient with the flapless technique and to instantly load the site after surgery (Figure 23-30).

### Conclusions

This study was intended to highlight the CBCT control importance during different surgical phases in implantology (Figure 31).

This imaging technique provides the surgeon with tridimensional orientation and helps to correct imprecise osteotomies: in fact this would not be possible using a steel pin and the classical approach with endo-oral XR (analogic/ digital/ phosphate sensor) or intra surgical OPTs.

This protocol makes it possible to have a safe approach to

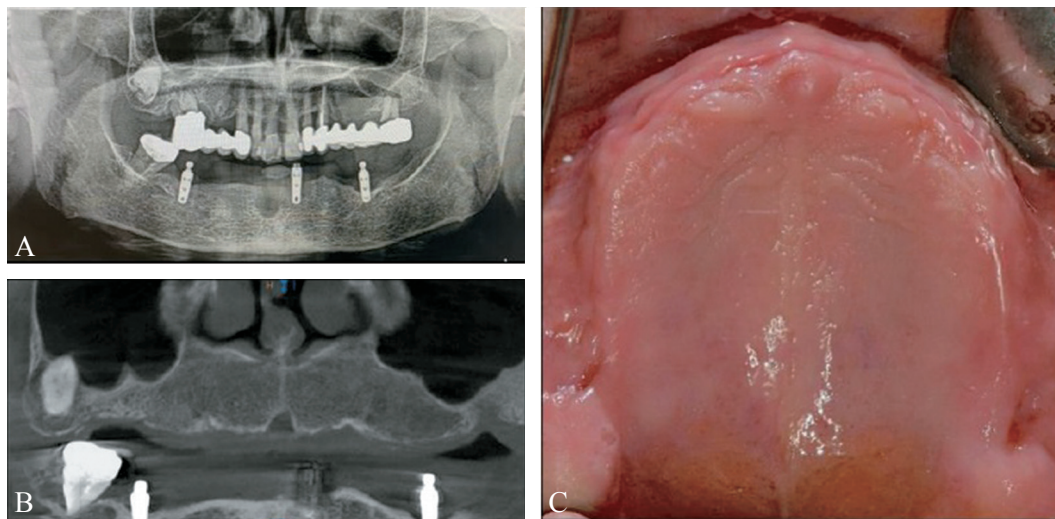


**Figure 23.**—A) Preoperative OPT; B) preoperative CBCT; C) preoperative picture.

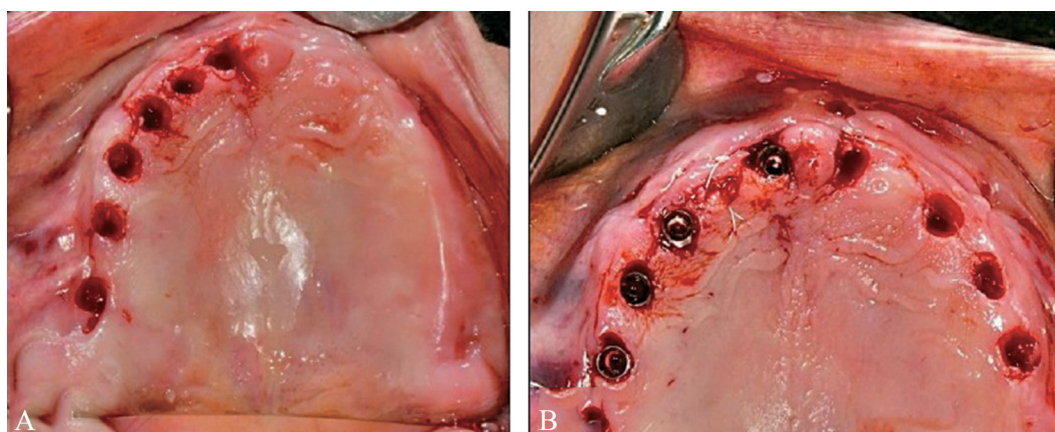


**Figure 24.**—A) Mucotomies in position 11, 12, 13, 15, 16, 17; B) Zimmer Biomet placed in position 11, 13, 15, 16. The gingival labrum replaced in position 12 and 17 and sutured with PTFE 4.0, after being conserved in a liquid solution with heparin. Mucotomies in position 21, 23, 25, 26.

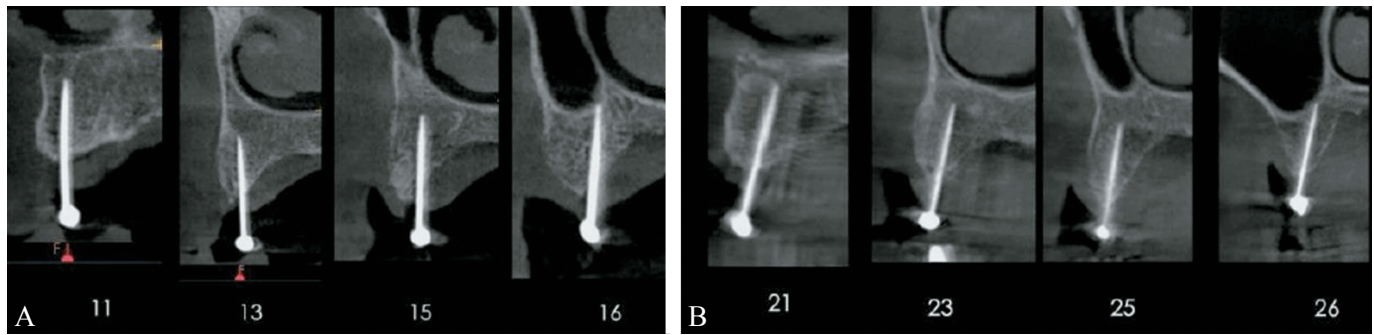


Figure 25.—Sectorial CBCT with reduced FOV in lowdose modality.

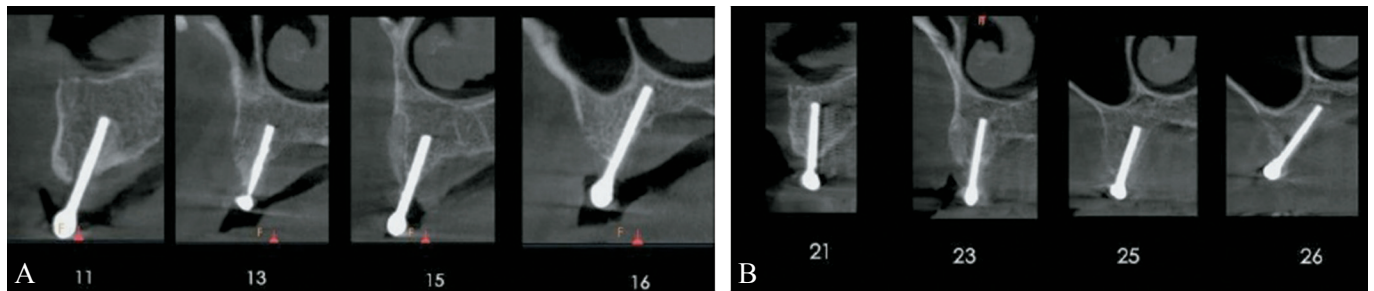


Figure 26.—Sectorial intraoperative CBCT in lowdose modality.

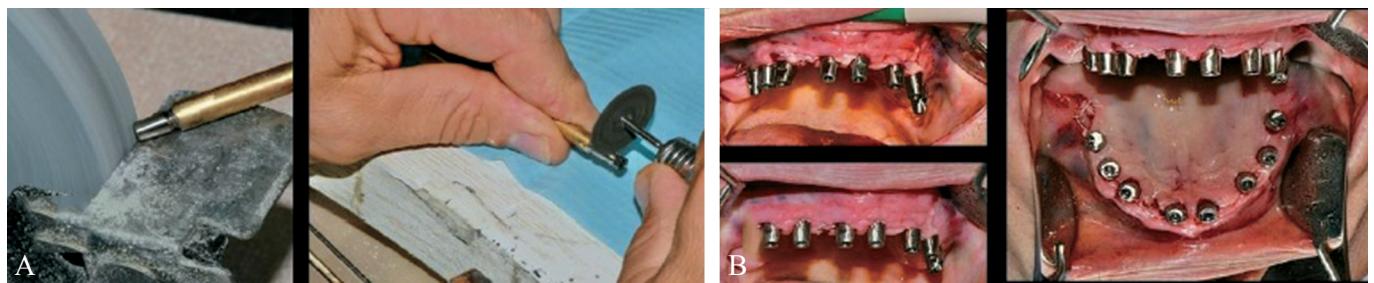


Figure 27.—A) Implant preparation; B) implant positioning.

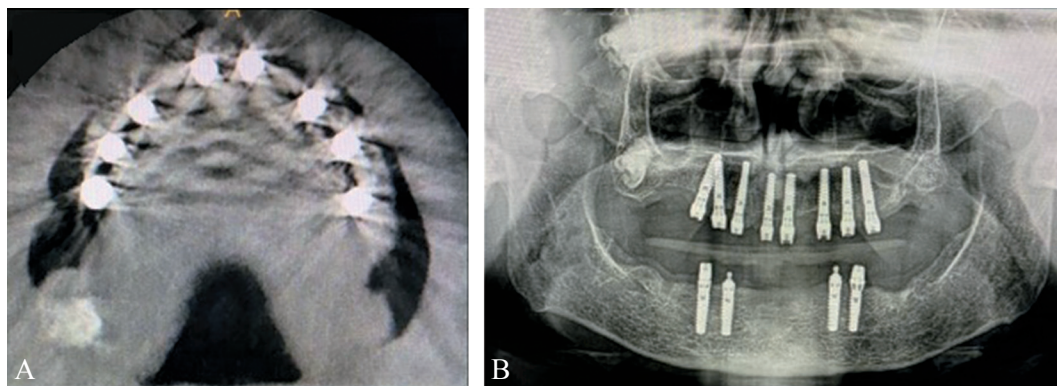


Figure 28.—A) panoramic CBCT carried out after surgery, showing the symmetrical position of the implants; B) post-operative OPT control showing apparent implantar overlap in position 15 and 16.

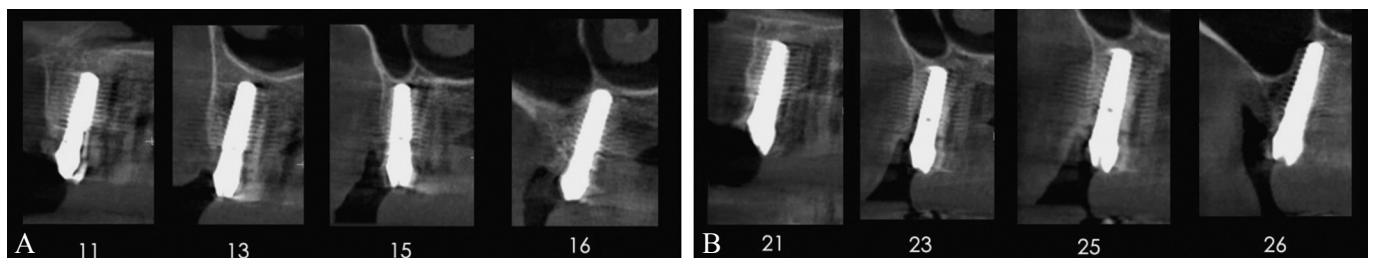


Figure 29.—This postoperative CBCT displays a Zimmer Biomet SPMB12 and a Zimmer Biomet SPMB14 pin placed respectively in position 16 and 26, respecting the sinu-maxillary bicortical structure.

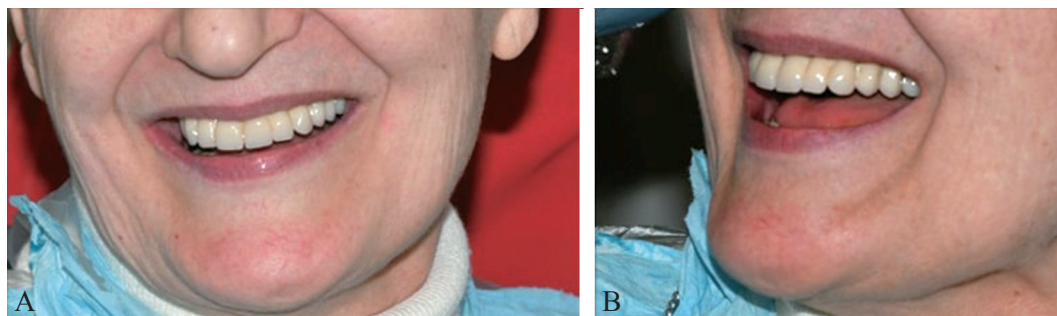


Figure 30.—Final result.

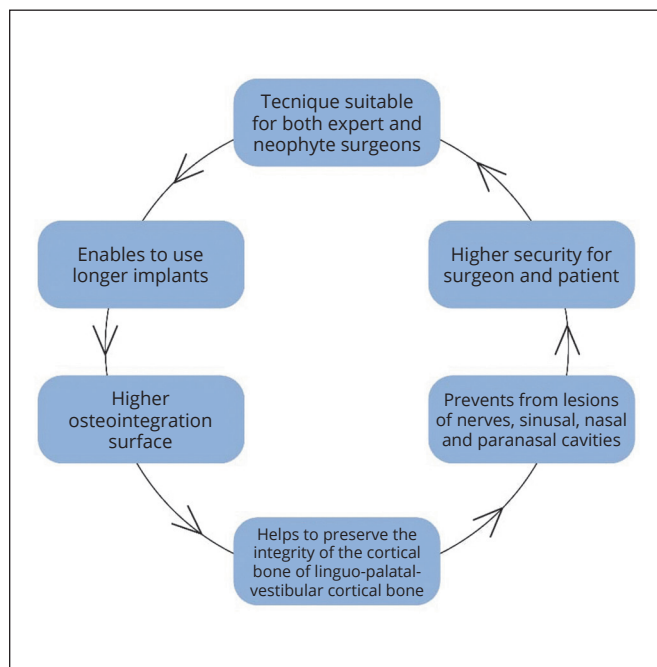


Figure 31.—A summary of all the achievements this protocol provides the surgeon with.

surgical sites that are difficult to reach due to their anatomical features, or to operate close to particular areas such as sinus cavities and paranasal and nasal cavities, moreover it enables to preserve the inferior alveolar nerve (IAN) and its integrity (Figure 32).

The intraoperative CBCT control facilitates to preserve the integrity of cortical bones in the vestibular, lingual and palatine area, also in cases that involve an implant placement characterized by an extremely inclined axis.<sup>1</sup> This way the implant can be performed by the use of simple UCLA (Universal Castable Long Aboutment) or MUA (Multi Unit Aboutment) (Figure 16, 19, 21, 22).

The CBCT osteotomy improves the success' predictability of implant surgery because it helps<sup>15</sup> a better use of the bone amount and makes possible to use implants that have a bigger osteointegration surface.

CBCT osteotomy provides the surgeon with the possibility to evaluate the milling cutter's inclination in the three planes of space.

CBCT technique makes implantology safer and more predictable, enabling the operator to achieve an optimal outcome in areas characterized by anatomical difficulties.<sup>16</sup>

The standard bidimensional X-ray controls performed by VRG, endo-oral X-rays and phosphate sensor enables to



Figure 32.—Pre and postoperative sectorial CBCT compared: here is shown how the implant was planned and realized respecting the inferior alveolar nerve's course.

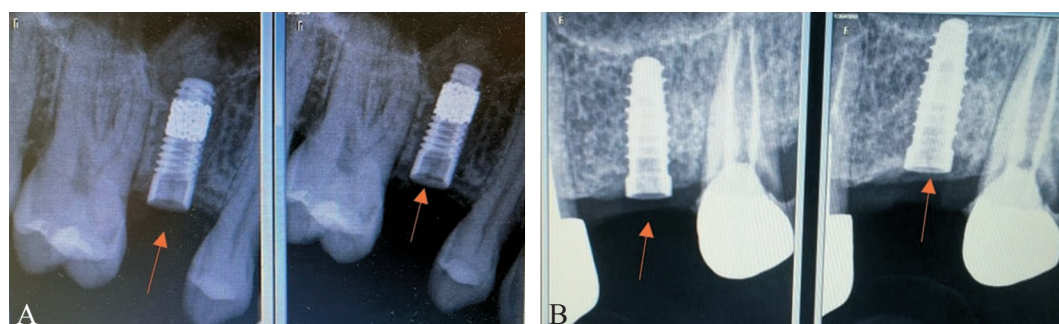
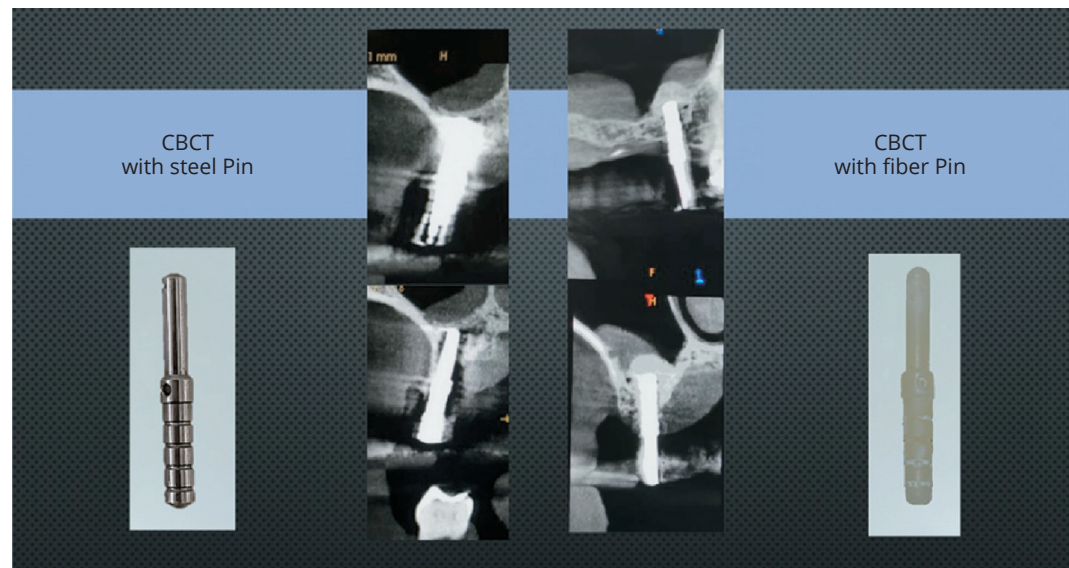


Figure 33.—Control VRG that highlights the necessity to adjust the implant insertion in the bony crest.



**Figure 34.**—Sectorial intraoperative CBCT compared: steel pin vs. fiber pin.

verify the osteotomy direction only in medio-distal direction, but the authors claim that it's pivotal to check whether the implant platform correctly placed (Figure 33). This must be assessed both on the recipient alveolar ridge and the implant features: structure, shape, machined neck and surface treatment.<sup>17</sup>

#### REFERENCES

1. Silveira-Neto N, Flores ME, De Carli JP, Costa MD, Matos FS, Paranhos LR, *et al.* Peri-implant assessment via cone beam computed tomography and digital periapical radiography: an ex vivo study. *Clinics (São Paulo)* 2017;72:708–13.
2. Oh TJ, Shotwell J, Billy E, Byun HY, Wang HL. Flapless implant surgery in the esthetic region: advantages and precautions. *Int J Periodontics Restorative Dent* 2007;27:27–33.
3. Benavides E, Rios HF, Ganz SD, An CH, Resnik R, Reardon GT, *et al.* Use of cone beam computed tomography in implant dentistry: the International Congress of Oral Implantologists consensus report. *Implant Dent* 2012;21:78–86.
4. Yepes JF, Al-Sabbagh M. Use of cone-beam computed tomography in early detection of implant failure. *Dent Clin North Am* 2015;59:41–56.
5. Tsai MT, He RT, Huang HL, Tu MG, Hsu JT. Effect of Scanning Resolution on the Prediction of Trabecular Bone Microarchitectures Using Dental Cone Beam Computed Tomography. *Diagnostics (Basel)* 2020;10:E368.
6. Gherlone E, Allegrini S, Annibali S, Baggi L, Barbato E, Barone A, *et al.* Raccomandazioni Cliniche in Odontostomatologia; 2017 [Internet]. Available from: [https://iris.unipa.it/retrieve/e3ad891d-377a-da0e-e053-3705fe0a2b96/C\\_17\\_publicazioni\\_2637\\_allegato.pdf](https://iris.unipa.it/retrieve/e3ad891d-377a-da0e-e053-3705fe0a2b96/C_17_publicazioni_2637_allegato.pdf) [cited 2022, Jul 15].
7. Pull Ter Gunne L, Wismeijer D. Accidental ingestion of an untethered instrument during implant surgery. *Int J Prosthodont* 2014;27:277–8.
8. Chan HL, Wang HL. Sinus pathology and anatomy in relation to complications in lateral window sinus augmentation. *Implant Dent* 2011;20:406–12.
9. Kato S, Omori Y, Kanayama M, Hirota A, Ferri M, Apaza Alccayhua-

man KA, *et al.* Sinus Mucosa Thickness Changes and Ostium Involvement after Maxillary Sinus Floor Elevation in Sinus with Septa. A Cone Beam Computed Tomography Study. *Dent J* 2021;9:82.

Thanks to the radiopaque pins applied in this protocol, it is possible to obtain clear and precise images without the artefact produced by metal bodies (Figure 34), in order to carry out intra operative controls with sectorial CBCT with reduced FOV<sup>18</sup> and exposing the patient to a low dose that equals to just 48 mGy/cm<sup>2</sup>.

10. Presidente IL, Repubblica D. LEGGE 4 ottobre 2019, n. 117. 2019:1-33.
11. Rabinowitz M, Glaser R. Cognitive Structure and Process in Highly Competent Performance. In: *The Gifted and the Talented: A Developmental Perspective*. Horowitz FD, O'Brien M, editors. Worcester, MA: American Psychological Association; 1986. p. 78-98.
12. Ufficiale G, Xxii A. Decreto legislativo del 31/07/2020 n. 101. 2020:141-2.
13. Zonca G, Pignoli E, Cesare Benetti C, Paglia L. La radioprotezione del paziente: dosi a confronto. *Il Dentista Moderno* 2008;26:62–78.
14. Lgs D. al comma 1, la lettera. 2000:532-755.
15. Sakka S, Coulthard P. Implant failure: etiology and complications. *Med Oral Patol Oral Cir Bucal* 2011;16:e42–4.
16. Herklotz I, Beuer F, Kunz A, Hildebrand D, Happe A. Navigation in implantology. *Int J Comput Dent* 2017;20:9–19.
17. Gilmozzi V. La diga di gomma in implantologia: due casi clinici. *Doctor Os*; 2016 [Internet]. Disponibile alla pagina. <https://www.doctoros.it/articoli-scientifici/implantologia/diga-di-gomma/> [citato il 21 luglio 2022].
18. Gibbs SJ. Effective dose equivalent and effective dose: comparison for common projections in oral and maxillofacial radiology. *Oral Surg Oral Med Oral Pathol Oral Radiol Endod* 2000;90:538–45.

**Conflicts of interest.**—The authors certify that there is no conflict of interest with any financial organization regarding the material discussed in the manuscript.

**Authors' contributions.**—All authors read and approved the final version of the manuscript.

**History.**—Manuscript accepted: July 12, 2022. - Manuscript revised: July 1, 2022. - Manuscript received: April 15, 2022.